International Journal of Membrane Science and Technology, 2023, Vol. 10, No. 1, pp 1395-1402

Enhancing The Adsorption Capacity of Commercial Kaolin for Efficient Removal of Lead Ions from Aqueous Solutions

Samer S. Abu-Alrub[1], Bandar A. Alyami[1*], Alhassan R. Alqarih[2], Bader A. Dunquwah[2], Elias A. Alhmari[2]

[1]Department of Pharmaceutical Chemistry, College of Pharmacy, Najran 11001, Najran University, Saudi Arabia; E-mail: ssaburub@nu.edu.sa

[2]College of Pharmacy, Najran 11001, Najran University, Saudi Arabia.

Abstract: The sorption of lead ions (Pb^{+2}) from aqueous solutions using commercial kaolin (KC) was investigated. The effects of various factors such as dosage, different pH media, different concentration, and temperature on the adsorption process were investigated. The Langmuir model was determined to fit the Pb^{+2}sorption model on KC. Langmuir model parameters q_m, K_L, and R^2, were found to be 31.2, 0.0014, and 0.9908 $mg.g^{-1}$ respectively. The q_{max} of the Pb^{+2} on KC was 31.2 $mg.g^{-1}$ at pH 5.7, 500 mg of KC, and 25°C. Free energy (ΔG), enthalpy (ΔH), and entropy (ΔS) were calculated to understand the nature of the sorption process. Negative ΔG, negative ΔH, and positive ΔS were found to indicate the adsorption process is non-spontaneous, exothermic, and random, respectively. A pseudo-second-order (PSO) model was followed for the adsorption process. The percentage extractions (%ER) found ranged from 102.5- 90.8 % for stimulation mineral water and tap water samples. This research provides valuable insights for the development of efficient and sustainable methods for water treatment and environmental remediation.

Keywords: Adsorption, Lead Ions, Commercial Kaolin, Adsorption Capacity, Adsorption Isotherm Models, Thermodynamic and Kinetics Models, and Environmental Treatment.

1. INTRODUCTION

The presence of heavy metals in aqueous media represents a significant risk to both ecosystems and human health [1, 2]. Among these heavy metals, lead (Pb) is of particular concern due to their widespread occurrence and detrimental effects[3, 4]. Efforts to reduce their negative influence have resulted in the investigation of several adsorbents for their removal from aqueous media[5, 6]. Pb is a hazardous metal that has been utilized in a variety of purposes for millennia, including construction, plumbing, batteries, and paints[7, 8]. However, the negative health impacts of lead exposure, particularly on children, have been noticed. Ingesting or breathing Pb can cause developmental difficulties, cognitive deficits, and damage to the nervous system and kidneys[9, 10].To remove Pb metals from drinking water and industrial effluent, several methods, such as adsorption, ion exchange, and filtering, are used[11, 12]. Adsorbents like as activated carbon, zeolites, and particular resins are often utilized due to their ability to effectively attract and retain Pb^{+2} [4, 13, 14]. Kaolin, a naturally occurring clay mineral, has received interest as a potential adsorbent for heavy metal removal due to its wide availability, low cost, and desirable physicochemical properties[15, 16]. Kaolin obtained from natural sources is a commercially available option for large-scale use in water treatment operations[17, 18]. The kinetics and thermodynamics of Pb ion adsorption onto various materials aid in the optimization and evaluation of treatment operations [17]. Contact time, initial metal concentration, pH, and temperature all have an impact on the adsorption capacity and removal efficiency (ER) of certain metals. The purpose of this research is to determine the adsorption capabilities of commercial kaolin (CK) for removing Pb ions from aqueous media. Batch adsorption parameters such as contact time, metal concentration, pH, and kaolin dose will be investigated to determine their impact on the adsorption process. Furthermore, commercial kaolin will be characterized to identify surface attributes like pore size distribution, specific surface area (SSA), and functional groups.

2. MATERIAL AND METHODS

2.1. Materials and Apparatus

Analytical-grade reagents were used throughout this project, and all materials were used directly out of the package. Pb $(NO_3)_2$ was purchased from Loba Chemie in India. Sigma Aldrich sells commercial kaolin with a total pore size and SSA of $0.0122 cm^3.g^{-1}$ and $10.702 m^2.g^{-1}$ respectively. Kwon et al. revealed the physiochemical characteristics of kaolin [19]. Because of the numerous bulky functional groups and high SSA (10.702 m2.g^{-1}) of Kaolin, It can absorb significant amounts of Pb^{+2} the chemical composition of the kaolin was determined, and the adsorbent was characterized at room temperature using a Fourier-transform infrared spectroscopy (FT-IR) Agilent, Cary 630. A Spectrophotometer Optima SP-3000 nano was used to determine the residual concentration of pb^{+2} in solutions (Japan), and an Ezdo pH meter (pp-201) was used to measure pH (Taiwan). A water bath shaker from Daihan Scientific in Korea was used to run this experiment.

2.2. Adsorption of the Pb^{+2}

The batch approach was used to research the Pb^{+2} adsorption characteristics. Fifty milliliters of the Pb^{+2} was combined with an adsorbent mass of CK, and the mixture was stirred for a predetermined amount of time. The remaining amount of Pb adsorbed by the CK could be determined by the difference between the initial and final concentrations after the final Pb^{+2} concentrations (Ce) in the aqueous solution were measured. Following the investigation described below, the effects of kaolin mass, Pb^{+2} concentration, contact time, pH, and temperature on Pb^{+2} adsorption were examined. At 300 nm, the Pb^{+2} concentrations that are still in solution were measured spectrophotometrically. Using a series of standard samples with concentrations between 1.8-57.5mM, a linear calibration curve was produced. With a correlation coefficient squared (R^2) of 0.9963, a linear calibration graph was produced. Every experiment was done in triplicate, and the standard deviation was used to calculate the measurement uncertainty, which was always judged to be less than 1.8%.

2.3. Effects of the Pb^{+2} on the Contact Time, Ph, Mass, And Temperature of The Adsorbent Of The Solution

The following approach was used to examine how contact time affected the adsorption of the Pb^{+2}: 50 mL solutions containing 29 mM of Pb^{+2} were first mixed with 500 mg of CK and stirred for periods ranging from 0 to 60 min and pH 5.7 at 25°C. The final Pb^{+2} concentrations were calculated. The agitation duration employed in following studies was determined to be 40 min, which was adequate to yield a reasonable value of the qe. The following adsorption investigations were conducted: In a 50 mL volumetric flask, 29 mM of Pb^{+2} concentrations were prepared. The final Pb^{+2} concentrations were calculated after stirring the flask for 40 min. The acidity of the solution's effect on Pb^{+2} adsorption, the effects of pH (1.0, 3.0, 5.7, 7.0, 8.2, 10.0, and 12.0), and CK mass (50 to 1000 mg) were investigated. The pH was checked at the start and end of the experiment, and it was then changed with either acid or base to reach the desired pH. Seven solutions with a pH of 7 and varying Pb^{+2} concentrations (1.8 to 57.5 mM) each received a mass of 500 mg of CK. The isotherm was studied at different temperatures (25, 30, 40, and 50 °C). The difference between the initial (C_i, mg.L^{-1}) and final (Ce, mg.L^{-1}) Pb^{+2} concentrations can be used to compute the concentration of adsorbed Pb^{+2} (q_e, mg.g^{-1}). Distribution coefficient Kd (L.g^{-1}) was used to express the Pb^{+2} absorption.

$$qe = \frac{(Ci-Ce)}{m} X\, V \ldots\ldots\ldots\ldots \text{ (1)}$$

$$Kd = \frac{qe}{Ce} \ldots\ldots\ldots\ldots\ldots\ldots\ldots\ldots \text{ (2)}$$

2.4. Effect of Pb^{+2} Concentrations

To study the impact of Pb^{+2} concentration, eight solutions were made, ranging in concentration from 1.8 to 57.5 mM, 500 mg of KC in 50 mL, and stirred for 40 min at 25 °C. The final Pb^{+2} concentrations were calculated.

3. RESULTS AND DISCUSSION

3.1. FT-IR Spectroscopy Investigation

Figure 1 shows the FT-IR spectra of commercial kaolin and commercial kaolin with Pb^{+2}. The peak found at 3300 cm^{-1} in the FTIR spectra of CK is most likely due to the presence of uncondensed -OH groups. The 1050 cm^{-1} peak is caused by Si-O stretching vibrations in the Si-OH bond. At 1550 cm^{-1}, asymmetric stretching vibrations of Si-O-Si bridges were found. Furthermore, the presence of Si-O-Al bonds is indicated by the peak at 990 cm^{-1} [20].Although the intensities of the peaks at 3300 cm^{-1} and 990 cm^{-1} were reduced slightly, the peak positions remained constant. This observation clearly shows that the Pb^{+2} is adsorbing onto the adsorbent by physical forces rather than chemical bonds.

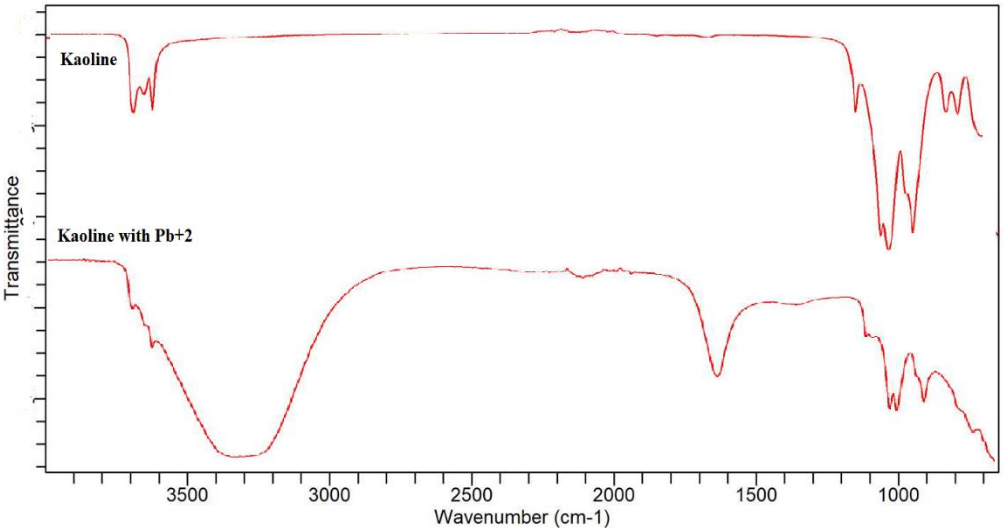

Figure1. FT-IR spectrum of the adsorbent kaolin before and after sorption with pb^{+2}.

3.2. Effect of Adsorbent Dose, Contact Time, pH, Initial Concentration, and Temperature of Solution

Figure 2a shows the results of experiments for Pb^{+2} uptake using different doses of CK varying from 50 to 1000 mg. The equilibrium uptake capacity (qe) of Pb^{+2} decreased as the adsorbent dosage increased and reached its maximum when 500 mg of CK was applied. Figure 2b shows the change in adsorption capacity (qe) as an indicator of contact time at a Pb^{+2} concentration of 29 µM. Pb^{+2} absorption was high during the first 40 minutes, followed by a decreasing rate of adsorption until equilibrium was obtained. After achieving equilibrium, there was no further adsorption of Pb^{+2}. Based on this data, a contact time of 40 minutes was determined to be optimal. Figure 2c shows the effect of solution pH on the equilibrium adsorption capacity (qe) under different conditions. The highest qe for CK was observed to increase as the pH increased. At pH 10, the highest qe value of 0.322 $mg.g^{-1}$ was found, which can be attributed to the precipitation of Pb^{+2} in the solution as $Pb(OH)_2$. Consequently, a pH of 5.7 was chosen for this investigation because it decreased the competition for active sites on CK between Pb^{+2} and H^+ ions. The electrostatic relationships that occur between the negatively charged surface of CK and the positively charged Pb^{+2} are encouraged by this pH state [21]. Figure 4d shows the effect of various initial Pb^{+2} concentrations ranging from 2 to 58 mM on the method of adsorption. The adsorption capacity of Pb^{+2} onto CK increased as the beginning concentration of Pb^{+2} increased from 15 mM to 58 mM, with qe values going from (0.029 to 0.264) $mg.g^{-1}$. This result highlights the significance of the starting concentration on adsorption capacity, indicating a strong correlation between the two variables. Figure 2e shows the relationship between the qe of Pb^{+2} and temperature. It is found that qe increases with increasing temperature, indicating an exothermic adsorption mechanism. As a result, higher temperatures enhance the adsorption of Pb^{+2} onto CK. Table 1 shows the estimated thermodynamic parameters, which include the free energy (ΔG), enthalpy (ΔH), and entropy (ΔS). Negative ΔG values indicate that Pb^{+2} sorption onto CK are feasible and spontaneous. Furthermore, the quantity of ΔG increases with increasing temperature, indicating a greater degree of spontaneity at higher temperatures. A positive ΔS value shows enhanced randomness at the solid/liquid interface during Pb^{+2} sorption onto CK. The negative value of ΔH confirms that Pb^{+2} sorption onto CK are exothermic. This investigation supports the conclusion that Pb^{+2} sorption onto CK is a physical adsorption process.

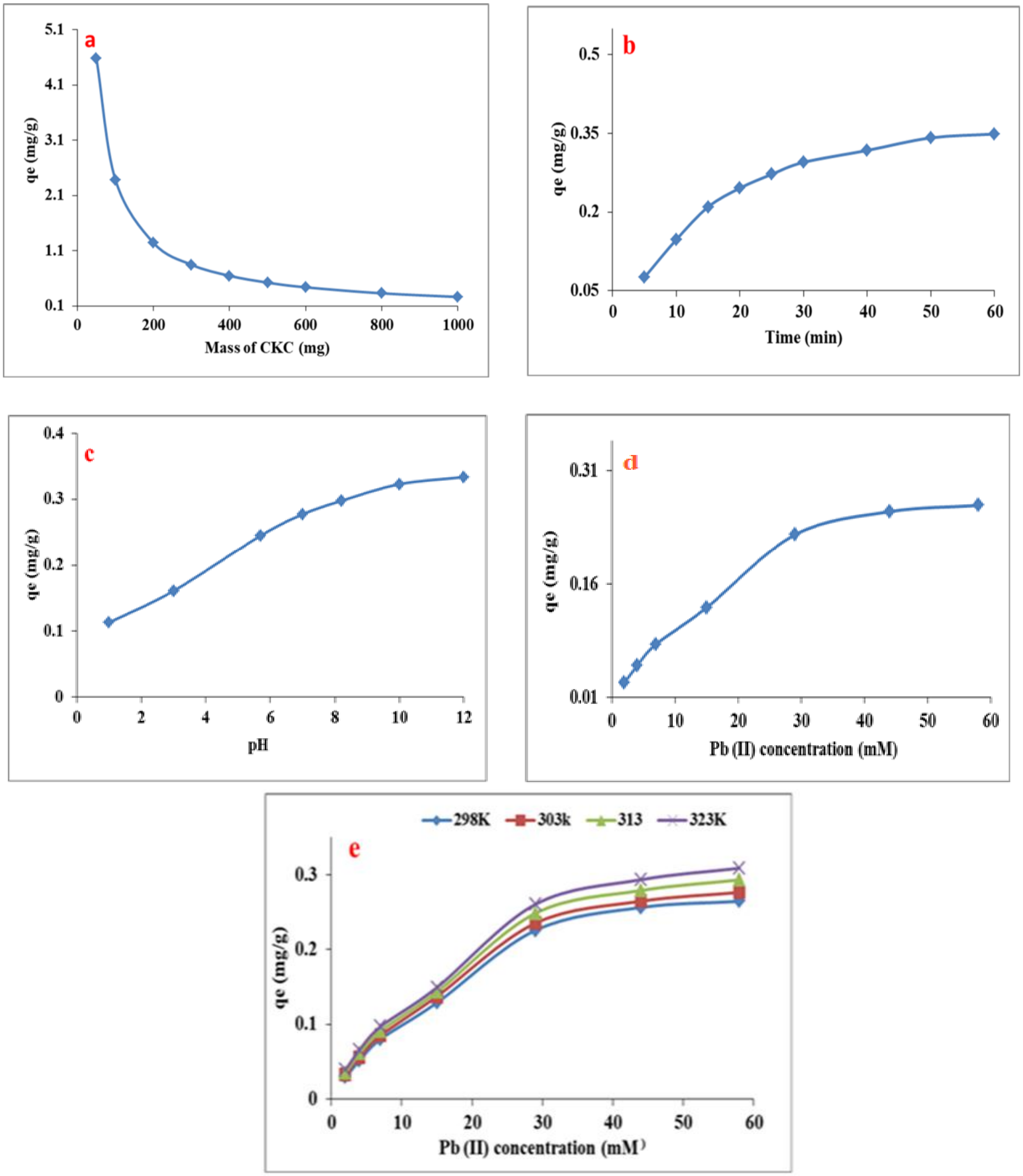

Figure2. Impact of mas of KC (a), contact time (b), pH (c), Pb (II) concertation (d) and temperature (e) on the equilibrium adsorption capacity (q_e) of Pb (II) onto KC.

Table1. Thermodynamic parameters for the sorption process

ΔH (KJ.mol^{-1})	ΔS (J.K^{-1}.mol^{-1})	ΔG (KJ.mol^{-1})			
		298 K	303 K	313 K	323K
-304.3	34.3	-10.5	-10.7	11.1	-11.4

3.3. Isotherms Adsorption Assessment

The adsorption isotherm shows the adsorption capacity (qe) of Pb^{+2} and KC adsorbent at equilibrium within the sorption process. The examination of isotherm models is important until the optimum model is determined to represent the adsorption process at various temperatures[22]. The Langmuir model indicates that the sorption process occurs at a homogenous active site on the adsorbent [23]. The Langmuir isotherm equation is shown as follows:

$$\frac{Ce}{qe} = \frac{1}{kl\ qm} + \frac{Ce}{qm} \text{………………….. (3)}$$

Where $Ce, qe, qm, V, and\ kl$ the final concentrations (mM), adsorption capacity (mg.g^{-1}), theoretical adsorption capacity, and constant isotherm Langmuir, respectively. The K$_d$ and q$_m$ values can be calculated by linearly plotting $\frac{Ce}{qe}$ vs. Ce. The Freundlich isotherm indicates that the adsorption process occurs between adsorption capacity and Pb^{+2} concentration on a heterogeneous absorbent surface at equilibrium [23]. As follows is the Freundlich equation:

$$qe = KfCe^{1/n} \text{………………….. (4)}$$

The plot of ln qe against ln C$_e$ was used to calculate the values of Kf and$1/n$ from the intercept and slope, respectively.

The Timken model predicts a decrease in the heat of adsorption for molecules in the layer as a result of the adsorption process [24]. The Temkin isotherm's linear form is represented as:

$$qe = BlnA + B\ lnCe \text{ …………… (5)}$$

Where $B, and\ A$ the heat of adsorption-related Temkin constant, and the constant of equilibrium binding (L.mg^{-1}), respectively. A Plot of qe vs $lnCe$ will show the constants A and B.

In Table 2, all the R^2 values and parameter constants acquired from the three models are listed. The values of R^2 in the Langmuir model were higher than the R^2 values in the Freundlich and Temkin models at different temperatures. Which demonstrated that the Langmuir model was the most suitable for describing the adsorption of Pb^{+2} on KC [25]. Indicating exothermic adsorption, the Kf shown increased with the temperature increased. The values of n were more than 1, which indicates the adsorption condition was acceptable [25].

Table2. Isotherm models parameters for the adsorption process

Mdole	25 ˚C	30 ˚C	40 ˚C	50 ˚C
Langmuir				
q$_m$	31.2	31.3	31.4	33.3
K$_L$	0.0014	0.0016	0.0029	0.0024
R^2	0.9908	0.9820	0.9896	0.9732
Freundlich				
K$_f$	29.5	25.6	22.2	21.6
n	1.7	1.8	1.9	3.3
R^2	0.8988	0.8117	0.7920	0.7677
Temkin				
A	0.071	0.072	0.005	0.056
B	0.001	0.003	0.005	0.016
R^2	0.9640	0.9181	0.8369	0.7249

3.4. Kinetics Assesment

To examine and determine the effectiveness and rate of adsorbate at equilibrium time, we studied the kinetics of adsorption. The PFO and PSO models were studied and examined to find the most suitable model for the experimental data from the sorption process of Pb^{+2} onto KC. The following formulas (6) and (7) were used to compute the values of k_1 and q_e ($mg.g^{-1}$) by plotting a graph of log (qe-qt) vs 't'(min), and values of k_2 and q_e ($mg.g^{-1}$) were founded by plotting t/q_e vs't' (min).

PFO model formula:

$$\log(qe - qt) = logqe - \left[\frac{k1}{2.303}\right] t \text{..........} \quad (6)$$

PSO model formula:

$$\frac{t}{qt} = \frac{1}{k2qe2} + t/qe \text{..........................} \quad (7)$$

Where qe and qt equal the quantity of Pb^{+2} adsorbed ($mg.g^{-1}$) at equilibrium and at any other time during the adsorption process, respectively. Table 3 showed R^2 values for the PFO and PSO models were 0.6675 and 9810 for Pb^{+2}. The qe (exp) values at PFO model did not match with the qe (cal) values, therefore, the PFO model does not fit with the adsorption of Pb^{+2} into KC. The value of qe (exp) was in agreement with the qe (cal). Table 3 indicating that PSO model is the suitable kinetic model for Pb^{+2} into KC. The adsorption process was controlled via chemisorption.

Table 3 Kinetic parameters for the adsorption process

C_i (mM)	q_{exp} ($mg.g^{-1}$)	PFO			PSO		
		$k1$	$qcal.$	R^2	$k2$	$qcal.$	R^2
29	5.5	$2.19X10^{-2}$	35.9	0.6675	$5.27X10^{-3}$	0.5	0.9924

3.5. The Pb^{+2} Adsorption Capacity of The CK Adsorbents Was Compared to Some Previous Reports.

Table 4 was used to compare the q_{max} of the CK adsorbents in this study to the effects of Pb^{+2} on CK adsorbent in previous reports. The results showed that the q_{max} varied depending on the used experimental conditions. The adsorption capacity of the Pb^{+2} in this study also varied compared to other CK adsorbents. Table 3 demonstrates that kaolin has notably high adsorption efficiency for Pb^{+2} when compared to all the adsorbents mentioned in the literature.

Table 4 The adsorption capacity (q_{max}) and an isotherm models of different adsorbents reported in the literature for the adsorption of Pb^{+2}.

Adsorbent	q_{max} ($mg.g^{-1}$)	Isotherm model	Ref.
Kaolinite	11.5	Langmuir	[26]
Zeolite	14.0	Langmuir	[27]
Celtic clay	18.1	Langmuir	[28]
Montmorillonite	31.1	Langmuir	[26]
Bentonite clay	9.9	Langmuir	[29]
Commercial kaolin	31.2	Langmuir	This study

3.6. Various Applications of Water Samples

The percentage of extraction recovery (%ER) of Pb^{2+} was determined in tap water samples and mineral water samples. The % ER ranged from 102.5– 95.8% and 102.3–90.8% in mineral water and tap water samples, respectively, as represented in Table 5.

Table 5 Percentage extraction recovery of Pb^{2+} from Mineral water samples and tap water samples

Sample	Added (mM)	Found (mM)	% ER ± SD
Mineral water	2	1.9	98.5±1.0
	6	6.1	101.2 ± 0.8
	10	9.7	97.3± 0.9
	30	3.1	102.5 ± 0.6
	50	47. 9	95.8± 0.5
Tap water	2	1.8	93.6± 0.9
	6	5.9	99.3± 0.9
	10	10.2	102.3±0.8
	30	29.5	98.4± 0.7
	50	45.4	90.8 ± 1.0

CONCLUSION

The present study investigated the adsorption of Pb^{+2} from aqueous solutions by commercial kaolin. The findings provide valuable insights into optimizing the adsorption capacity of KC for the removal of lead ions. Based on the experimental results, several factors were identified that can be manipulated to enhance the adsorption capacity. The q_{max} of the Pb^{+2} on KC was 31.17mg.g^{-1} at pH 5.7, 500 mg of KC, and 25°C. The sorption isotherm data were linked to the Langmuir model using an adsorption isotherm for Pb^{+2} on KC. The PSO kinetic model was obeyed for the adsorption of Pb^{+2} with KC. The results of this study demonstrate the potential of commercial kaolin as a reliable and cost-effective adsorbent for the removal of lead ions. These findings contribute to the development of optimized protocols for water treatment and environmental remediation, aiming to mitigate the harmful effects of lead contamination.

Acknowledgments

The authors are thankful to the Deanship of Scientific Research at Najran University for funding this work under the Future Funding program grant code (NU/SRP/MRC/12/1).

Conflict of Interest

The authors declare no conflict of interest

REFERENCE

[1] S.E. Bailey, T.J. Olin, R.M. Bricka, D.D. Adrian, A review of potentially low-cost sorbents for heavy metals, Water research, 33 (1999) 2469-2479.

[2] N. Ünlü, M. Ersoz, Adsorption characteristics of heavy metal ions onto a low cost biopolymeric sorbent from aqueous solutions, Journal of hazardous materials, 136 (2006) 272-280.

[3] M.-q. Jiang, X.-y. Jin, X.-Q. Lu, Z.-l. Chen, Adsorption of Pb (II), Cd (II), Ni (II) and Cu (II) onto natural kaolinite clay, Desalination, 252 (2010) 33-39.

[4] W.W. Ngah, M.M. Hanafiah, Removal of heavy metal ions from wastewater by chemically modified plant wastes as adsorbents: a review, Bioresource technology, 99 (2008) 3935-3948.

[5] K. Kadirvelu, M. Kavipriya, C. Karthika, M. Radhika, N. Vennilamani, S. Pattabhi, Utilization of various agricultural wastes for activated carbon preparation and application for the removal of dyes and metal ions from aqueous solutions, Bioresource technology, 87 (2003) 129-132.

[6] B. Singh, Heavy metals in soils: sources, chemical reaction and forms. In 'GeoEnvironment: proceedings of the 2nd Australia and New Zealand conference on environmental geotechnics'. Newcastle, New South Wales, (2001).

[7] U. Atsdr, Toxicological profile for lead (Atlanta, GA: US Department of Health and Human Services, Agency for Toxic Substances and Disease Registry (ATSDR), Public Health Service), US EPA Air quality criteria for lead, (2007).

[8] T. Sanders, Y. Liu, V. Buchner, P.B. Tchounwou, Neurotoxic effects and biomarkers of lead exposure: a review, Reviews on environmental health, 24 (2009) 15-46.

[9] M. Lustberg, E. Silbergeld, Blood lead levels and mortality, Archives of internal medicine, 162 (2002) 2443-2449.

[10] V.M. Weaver, B.G. Jaar, B.S. Schwartz, A.C. Todd, K.-D. Ahn, S.-S. Lee, J. Wen, P.J. Parsons, B.-K. Lee, Associations among lead dose biomarkers, uric acid, and renal function in Korean lead workers, Environmental health perspectives, 113 (2005) 36-42.

[11] Z. Saadi, R. Saadi, R. Fazaeli, Fixed-bed adsorption dynamics of Pb (II) adsorption from aqueous solution using nanostructured γ-alumina, Journal of Nanostructure in Chemistry, 3 (2013) 1-8.

[12] H.B. Bradl, Adsorption of heavy metal ions on soils and soils constituents, Journal of colloid interface science, 277 (2004) 1-18.

[13] N.V. Medvidović, J. Perić, M. Trgo, Column performance in lead removal from aqueous solutions by fixed bed of natural zeolite–clinoptilolite, Separation Purification Technology, 49 (2006) 237-244.

[14] Y.-H. Li, Z. Di, J. Ding, D. Wu, Z. Luan, Y. Zhu, Adsorption thermodynamic, kinetic and desorption studies of Pb2+ on carbon nanotubes, Water research, 39 (2005) 605-609.

[15] K.G. Bhattacharyya, S.S. Gupta, Adsorption of a few heavy metals on natural and modified kaolinite and montmorillonite: a review, Advances in colloid interface science, 140 (2008) 114-131.

[16] G. Suraj, C. Iyer, M. Lalithambika, Adsorption of cadmium and copper by modified kaolinites, Applied Clay Science, 13 (1998) 293-306.

[17] A. Awwad, M. Amer, M. Al-aqarbeh, TiO2-kaolinite nanocomposite prepared from the Jordanian Kaolin clay: Adsorption and thermodynamics of Pb (II) and Cd (II) ions in aqueous solution, Chemistry International, (2020).

[18] J.-B. Chai, P.-I. Au, N.M. Mubarak, M. Khalid, W.P.-Q. Ng, P. Jagadish, R. Walvekar, E.C. Abdullah, Adsorption of heavy metal from industrial wastewater onto low-cost Malaysian kaolin clay–based adsorbent, Environmental Science Pollution Research, 27 (2020) 13949-13962.

[19] S. Kwon, H. Hwang, Y.J.C. Lee, Effect of pressure treatment on the specific surface area in kaolin group minerals, 9 (2019) 528.

[20] M. Roulia, K. Chassapis, J. Kapoutsis, E. Kamitsos, T. Savvidis, Influence of thermal treatment on the water release and the glassy structure of perlite, Journal of materials science, 41 (2006) 5870-5881.

[21] I. Ogbu, K. Akpomie, A. Osunkunle, S.J.B.J.o.S. Eze, I. Research, Sawdust-kaolinite composite as efficient sorbent for heavy metal ions, 54 (2019) 99-110.

[22] B. Royer, N.F. Cardoso, E.C. Lima, J.C. Vaghetti, N.M. Simon, T. Calvete, R.C.J.J.o.h.m. Veses, Applications of Brazilian pine-fruit shell in natural and carbonized forms as adsorbents to removal of methylene blue from aqueous solutions—Kinetic and equilibrium study, 164 (2009) 1213-1222.

[23] A. Afkhami, T. Madrakian, A.J.D. Amini, Mo (VI) and W (VI) removal from water samples by acid-treated high area carbon cloth, 243 (2009) 258-264.

[24] I.D. Mall, V.C. Srivastava, N.K. Agarwal, I.M.J.C. Mishra, Removal of congo red from aqueous solution by bagasse fly ash and activated carbon: kinetic study and equilibrium isotherm analyses, 61 (2005) 492-501.

[25] F.J.A.W.S. Togue Kamga, Modeling adsorption mechanism of paraquat onto Ayous (Triplochiton scleroxylon) wood sawdust, 9 (2019) 1.

[26] S.S. Gupta, K.G. Bhattacharyya, Interaction of metal ions with clays: I. A case study with Pb (II), Applied clay science, 30 (2005) 199-208.

[27] A. Rakhym, G. Seilkhanova, T. Kurmanbayeva, Adsorption of lead (II) ions from water solutions with natural zeolite and chamotte clay, Materials Today: Proceedings, 31 (2020) 482-485.

[28] A. Sarı, M. Tuzen, M. Soylak, Adsorption of Pb (II) and Cr (III) from aqueous solution on Celtek clay, Journal of Hazardous Materials, 144 (2007) 41-46.

[29] R.A.M.a.S.S. Mohammed, Kinetic and thermodynamic study of adsorption of an industrial food dye using Iraqi clay, Journal of Population Therapeutics & Clinical Pharmacology, 30 (2023) e279–e287.

DOI: https://doi.org/10.15379/ijmst.v10i1.2887